Murawski, A., Vorogushyn, S., Bürger, G., Gerlitz, L., Merz, B. (2018): Do Changing Weather Types Explain Observed Climatic Trends in the Rhine Basin? An Analysis of Within- and Between-Type Changes. - *Journal of Geophysical Research*, *123*, 3, pp. 1562—1584.

DOI: http://doi.org/10.1002/2017JD026654

AGU PUBLICATIONS

JGR

Journal of Geophysical Research: Atmospheres

RESEARCH ARTICLE

10.1002/2017JD026654

Do Changing Weather Types Explain Observed Climatic Trends in the Rhine Basin? An Analysis of Within- and Between-Type Changes

Aline Murawski[1,2,3], Sergiy Vorogushyn[1], Gerd Bürger[3,4], Lars Gerlitz[1], and Bruno Merz[1,3]

[1]GFZ German Research Centre for Geosciences, Potsdam, Germany, [2]Institute of Hydraulic Engineering and Water Resources Management, Vienna University of Technology, Vienna, Austria, [3]Institute of Earth and Environmental Science, University of Potsdam, Potsdam, Germany, [4]Institute of Meteorology, FU Berlin, Berlin, Germany

Key Points:
- Analysed large (490 stations) and long (111 years) data set for Rhine catchment
- Stationarity of weather pattern characteristics using multiple periods has been tested for the purpose of downscaling
- Changes in temperature and precipitation are mainly related to changes in the occurrence of patterns

Supporting Information:
- Supporting Information S1
- Data Set S1
- Figure S1
- Figure S2
- Figure S3
- Figure S4
- Figure S5
- Figure S6
- Figure S7
- Figure S8

Correspondence to:
A. Murawski,
murawski@gfz-potsdam.de

Citation:
Murawski, A., Vorogushyn, S., Bürger, G., Gerlitz, L., & Merz, B. (2018). Do changing weather types explain observed climatic trends in the Rhine basin? An analysis of within- and between-type changes. *Journal of Geophysical Research: Atmospheres*, *123*, 1562–1584. https://doi.org/10.1002/2017JD026654

Received 14 FEB 2017
Accepted 6 JAN 2018
Accepted article online 19 JAN 2018
Published online 7 FEB 2018

Abstract For attributing hydrological changes to anthropogenic climate change, catchment models are driven by climate model output. A widespread approach to bridge the spatial gap between global climate and hydrological catchment models is to use a weather generator conditioned on weather patterns (WPs). This approach assumes that changes in local climate are characterized by between-type changes of patterns. In this study we test this assumption by analyzing a previously developed WP classification for the Rhine basin, which is based on dynamic and thermodynamic variables. We quantify changes in pattern characteristics and associated climatic properties. The amount of between- and within-type changes is investigated by comparing observed trends to trends resulting solely from WP occurrence. To overcome uncertainties in trend detection resulting from the selected time period, all possible periods in 1901–2010 with a minimum length of 31 years are analyzed. Increasing frequency is found for some patterns associated with high precipitation, although the trend sign highly depends on the considered period. Trends and interannual variations of WP frequencies are related to the long-term variability of large-scale circulation modes. Long-term WP internal warming is evident for summer patterns and enhanced warming for spring/autumn patterns since the 1970s. Observed trends in temperature and partly in precipitation are mainly associated with frequency changes of specific WPs, but some amount of within-type changes remains. The classification can be used for downscaling of past changes considering this limitation, but the inclusion of thermodynamic variables into the classification impedes the downscaling of future climate projections.

1. Introduction

Understanding how hydrological change is linked to human-induced climate change is important for water resources management and climate adaptation. Various studies investigate the variability and change of hydrologically relevant climate variables for central Europe. Specific regional scale weather patterns (WPs) or large-scale circulation modes have been found to be related with hydrometeorological extremes; see, for example, Steirou et al. (2017) for a review. However, the length of observational time series (mostly below 100 years) is often insufficient to investigate the statistical relationships between climatic conditions and rare flood events. A widespread approach to link hydrological extremes to variations of the large-scale circulation is to force spatially distributed hydrological models at the catchment scale with the output from global climate models. To bridge the spatial gap between coarse global climate models and catchment models, numerous downscaling approaches have been developed; see, for example, Maraun et al. (2010) for a review. In particular, the approach of conditioning a weather generator (WGN) by means of climate model output data offers the possibility to generate very long (≥10,000 years) synthetic time series at several locations considering the spatial correlation structure of meteorological variables (Elshamy et al., 2006; Fatichi et al., 2011; Fowler et al., 2000, 2005; Hewitson & Crane, 2006; Kilsby et al., 2007; Kim et al., 2016; Lu et al., 2015; Steinschneider & Brown, 2013; te Linde et al., 2010). This approach is particularly suitable for a robust estimation of changes in floods since their statistical moments can be better captured using very long time series of climate time series.

WGNs produce sequences of stationary weather. Hence, to be useful for climate change impact investigation, they need to be conditioned on large-scale climate fields as simulated, for example, by climate models. A natural way to do this is to decompose the large-scale variability into a discrete and finite set of dominant

weather types, within which the weather is considered stationary. This can be done subjectively by inspecting synoptic weather charts ("Großwetterlagen") (e.g., Brezowsky & Hess, 1952) or objectively by using automated statistical tools such as clustering.

Recently, an optimal weather classification comprising 40 classes has been developed and validated for the Rhine catchment in Murawski et al. (2016). This classification is based on ECMWF's (European Centre for Medium-Range Weather Forecasts) atmospheric reanalysis of the 20th century (ERA-20C) data of dynamic (sea level pressure) and thermodynamic (near-surface temperature, specific humidity) fields and utilizes the state-of-the-art SANDRA algorithm (Philipp, 2009; Philipp et al., 2007). In order to utilize a WP classification for downscaling applications, a robust statistical relationship between WPs and local scale observations is required; that is, the variance explained by the clustering (or rather the fraction of local between-type variance) should be substantial. If that fraction is large enough, local variability is believed to be sufficiently conditioned on the large-scale climate fields. To be applied to simulated climate fields, however, two more conditions are required to hold: (i) the climate models reliably simulate the statistics of the weather types and (ii) the link between the weather types and the local weather remains valid.

The ability of the classification to stratify local climate variables (such as temperature and precipitation) has been proven in Murawski et al. (2016). We found the majority of global climate models from the coupled model intercomparison project 5 (Taylor et al., 2012) to be capable of reproducing the WP climatology of the ERA-20C reanalysis data. In this follow-up paper we tackle the last point, (ii), about the stability of the link between weather types and local variables that is required to drive a hydrological model. Therefore, we conduct a systematic analysis of trends in WP frequencies and WP internal characteristics and investigate whether observed trends in local climate variables can be attributed to changes in WP compositions. We explicitly emphasize that the classification of Murawski et al. (2016) aims at optimizing the amount of explained variance. It does not aim at separating between dynamical and thermodynamic fractions in past climate observations (Shepherd, 2014), as it includes both dynamic and thermodynamic variables. The classification is tested for the assumption that observed temporal changes can be fully explained by between-type changes. This is a prerequisite for using it for WGN-based downscaling.

The main goal of the ERA-20C reanalysis project was to create a century-long set of atmospheric fields that are as immune as possible to artificial trends induced by the growing data coverage; we assume that large-scale trends are well captured by the input data. This is further supported by Poli et al. (2013), who show that ERA-20C trends are particularly reliable near the surface of the northern hemispheric extratropics.

Climate change might manifest itself in WPs in two different manners. On the one hand, the occurrence of WPs might change, reflected in changes in the frequency of patterns (e.g., dry patterns occur more often), in the seasonality (e.g., a summer pattern being observed already in spring), or in the persistence of patterns (e.g., a dry and warm pattern occurs for longer periods). These changes are termed between-type changes. On the other hand, within-type changes can occur; that is, the characteristics of local climate variables for a given WP can change (e.g., more precipitation). The assumption of a stationary link between WPs and local climate requires that climate change manifests only as between-type change. Although there are numerous studies that have relied on a stationary link between WPs and local climate, previous analyses indicated that this assumption might be violated (Widmann & Schär, 1997). Hewitson and Crane (2006) pointed out that land use and land cover changes could affect local climate and thus modify the link to WPs. Jacobeit et al. (2003) detected within-type changes in some circulation types over Europe. Beck et al. (2007) found that large parts of the climate variability between 1780 and 1995 in central Europe could not be explained by variability in WPs. Cahynová and Huth (2010) applied decomposition of climatic differences and the hypothetical trend methodology to differentiate the role of frequency and within-type changes on trends in six climate variables over the Czech Republic. Both decomposition techniques, of which we only use the latter here, indicated that a relatively small share of changes could be explained by frequency changes in the period 1961–1998. Küttel et al. (2011) indicated a strong role of within-type changes for changes in winter temperature and precipitation in Eastern Europe and Scandinavia by comparing multiple 50 year periods back to 1750. Also, Fleig et al. (2015) analyzed the role of frequency and within-type changes on monthly temperature and precipitation trends in Europe using the hypothetical trend technique. The relative share of frequency changes was found to vary strongly between 0 and 100% depending on the month and particular area within the European domain. Haberlandt et al. (2015) investigated the stationarity of the WP-precipitation link in a modeling study based on ECHAM/REMO climate model simulations and stochastic WGN experiments. They concluded

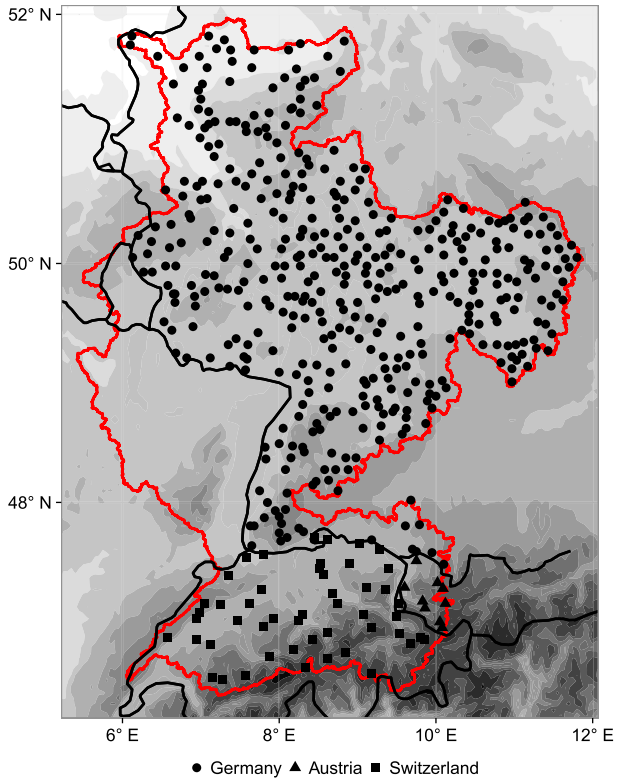

Figure 1. Locations of climate stations used. Red line shows Rhine catchment; black lines denote state borders. Background shading from light gray (low areas) to dark gray (high altitudes).

that the change in pattern frequency was not able to fully explain the change in future simulated total precipitation change.

This study extends the discussion on the stationarity of the WP-local climate link in two ways. First, previous studies indicating nonstationarity used mainly circulation variables for classification. While such classifications are able to clearly separate between dynamic and thermodynamic changes, they might insufficiently stratify local climate variables like temperature and precipitation and thus lead to within-type variability, thus impeding the application of a WGN based on WPs. To our knowledge only a few studies additionally consider other atmospheric variables to improve the discrimination of weather variables (Enke et al., 2005; Fleig et al., 2015). We address the question if a classification based on mean sea level pressure, temperature, and humidity is able to reduce within-type variability of WPs. Second, our analysis uses the idea of multiple trends, where all possible periods with a minimum length of 31 years are investigated. Since temporal changes are typically very sensitive to the selection of the start and end years of the time series, the multiple trend approach gives an indication of the robustness of the results.

In the following we introduce and interpret our WP classification with particular focus on classes associated with dry and moist conditions in the Rhine catchment. Typical characteristics, that is, the spatial distribution of sea level pressure, temperature, and humidity are illustrated for each WP. Relationships with well-known circulation indices (such as the North Atlantic Oscillation (NAO)) are analyzed, which allows the interpretation of WPs, their frequencies, and changes from a large-scale perspective. Subsequently, trends in frequency, seasonality, and persistence of WPs are analyzed and compared with changes of large-scale circulation indices. Within-type changes in four meteorological variables based on homogenized daily observation series at 490 climate stations over the 110 year period 1901–2010 are quantified. Finally, the relative contribution of frequency-related changes in explaining trends in selected meteorological variables is estimated.

2. Data and WP Classification

A previously developed WP classification (Murawski et al., 2016) is tested for stationarity of the link between patterns and associated climate variables. The classification uses mean sea level pressure, 2 m temperature, and specific humidity from the ERA-20C reanalysis (Poli et al., 2013) in the period 1900–2010 (explained variation of the input fields: 0.82). It covers the spatial domain 3–26°E/43–58°N with 40 classes/patterns and was optimized in terms of variables used for classification, spatial domain, and number of classes, to provide the best stratification of local climate variables. The ensemble mean of ERA-20C was used here only; thus, no conclusions regarding the uncertainty due to the reanalysis are possible. Due to the integration of dynamic (sea level pressure) and thermodynamic variables (temperature and specific humidity), the classification identifies WPs, characterized by anomalous pressure patters (and associated circulation modes) and specific thermal and hygric conditions. While major circulation patterns can be observed during the entire year, temperature and humidity feature a distinct seasonal cycle, enabling a continuous classification throughout the year and an assignment of WPs to individual seasons. The regional scale weather conditions for each WP are analyzed in terms of daily mean precipitation, temperature, relative humidity, and global shortwave radiation (hereafter referred to as PREC, T_{av}, RH, and RAD). Each pattern shows a clear seasonality of occurrence; thus, we can assign winter, summer, and spring/autumn patterns.

The analysis is based on 490 stations in the Rhine catchment for the period 1901–2010 (432 stations for the German part, 9 stations for Austria, and 49 stations for Switzerland and Liechtenstein; Figure 1). The station data were collected from the national meteorological services. Data processing and quality control was performed by the Potsdam Institute for Climate Impact Research (PIK) (Österle, Gerstengarbe, & Werner, 2006; Österle, Werner, & Gerstengarbe, 2006; Österle et al., 2016). This data set includes global shortwave radiation

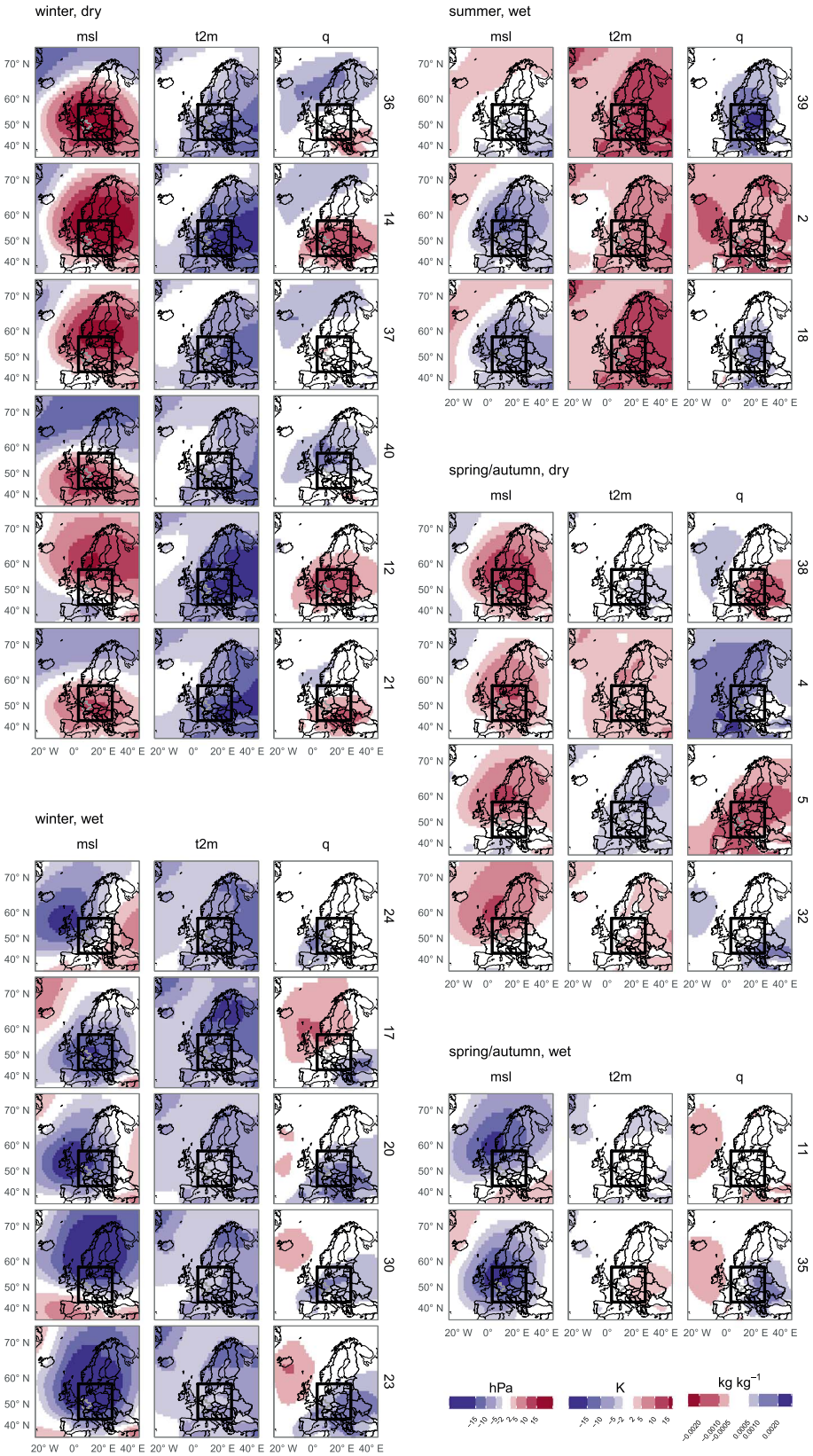

Figure 2. Centroids of patterns (wet and dry patterns only) expressed as anomalies (deviation from the overall mean (mean sea level pressure, msl; 2 m temperature, t2m), or the mean of the season's months only (specific humidity, *q*)). Black rectangle denotes the domain used for classification; gray outline indicates the Rhine catchment.

that was inferred from sunshine duration following Österle (2001) if not directly available. To date, no station data for the French part of the Rhine catchment are available. A more detailed description of the data set and the homogenization process is given in the supporting information.

Figure 2 illustrates the spatial distribution of sea level pressure, temperature, and humidity for WPs featuring exceptionally dry or moist conditions over the Rhine catchment (a complete overview of all WPs is provided in the supporting information). Dry conditions include all days with mean precipitation sums (calculated as a spatial mean over all stations) below the 25% quantile; moist conditions comprise days above the 75% quantile of the empirical distribution. In general, moist conditions are characterized by significantly negative pressure anomalies over central Europe, Scandinavia, and/or the western North Atlantic Ocean. The Rhine catchment is either located in the core region of the low-pressure cell or at its southern/southeastern edge. The associated cyclonic circulation pattern is accompanied by enhanced westerly moisture fluxes resulting in positive moisture anomalies over vast parts of central and southern Europe. The temperature anomalies of moist WPs follow the seasonal cycle. In contrast, dry conditions (for all seasons) depict strong positive pressure anomalies over Scandinavia and/or central Europe, triggering an anticyclonic circulation pattern. WPs featuring positive pressure anomalies over central Europe (WPs 21, 36, and 40) are associated with a direct blocking of the prevailing westerly flow and precipitation suppressing subsidence over the Rhine catchment. WPs characterized by a high-pressure center over Scandinavia (WPs 5, 12, 14, 32, 37, and 38) provoke an anticyclonic circulation over northern Europe. The Rhine is located at its southern edge and thus is under influence of northeasterly winds, advecting cold and dry air masses. Dry WPs are distinctly more often observed during winter than during all other seasons and are often accompanied with an intrusion of continental cold air, as represented by strongly negative temperature anomalies (e.g., in WPs 12 and 14).

3. Methods

3.1. Relationship of WPs and Large-Scale Circulation Modes

In order to identify large-scale atmospheric mechanisms favoring the occurrence of particular WPs and to relate trends of WP frequencies to changes of northern hemispheric circulation modes, we investigate the relationship between WP frequencies and well-known teleconnection indices.

As potential large-scale drivers, we consider monthly time series of the NAO, Scandinavian pattern (SCA), east Atlantic pattern (EA), and east Atlantic/western Russia pattern (EAWR) for the period 1950–2010. These are based on a rotated principal component analysis of 500 hPa geopotential height (GPH) fields (Barnston & Livezey, 1987) and represent leading (statistically independent) circulation modes over a domain north of 20°N. Positive and negative phases of each circulation mode are accompanied by specific large-scale pressure patterns and associated moisture fluxes. The NAO is characterized by two centers of action over the North Atlantic (Iceland Low) and the subtropical Atlantic (Azores High) and represents the strength of the meridional pressure gradient over the North Atlantic/European domain. Its positive phase features negative pressure anomalies over the North Atlantic and Scandinavia and positive anomalies over southern Europe and is accompanied by a northward shift of westerly moisture fluxes. Positive (negative) precipitation anomalies during the positive NAO phase have been frequently reported for northern Europe (the Mediterranean) (Steirou et al., 2017; Uvo, 2003). SCA is associated with strongly positive GPH anomalies over Scandinavia and is known to reflect blocking situations over northern and central Europe, accompanied by negative precipitation anomalies (Bueh & Nakamura, 2007; Comas-Bru & McDermott, 2014). EA is frequently referred to as a southward shifted NAO with its major center of action over the British Isles. Positive (negative) precipitation anomalies over northern Europe (the Mediterranean) are characteristic during its positive phase. EAWR features a dipole like pattern of GPH anomalies between central Europe and Russia. The positive phase is associated with strongly positive anomalies over Europe, which is accompanied by an anticyclonic circulation pattern and a southward deflection of westerly moisture fluxes (Krichak & Alpert, 2005).

We conduct a systematic spearman correlation analysis of WP frequencies with well-known teleconnection indices at a monthly scale; that is, the time series of WP frequencies are correlated with the mean state of any index, and correlations are tested for significance (t test, $\alpha = 0.1$) for each month of the year, respectively. Positive (negative) correlations indicate an increased (decreased) WP frequency during the positive phase of the considered index. The circulation modes are obtained from NOAA (http://www.cpc.ncep.noaa.gov/data/teledoc/telecontents.shtml).

With the aim of relating potential changes of WP frequencies to changes (or multidecadal variations) of large-scale circulation modes, a trend analysis for multiple periods is performed for the teleconnection indices and for each WP respectively (see section 3.2 for methodological details).

3.2. Trend Detection Methods

The fundamental assumption of WP-based downscaling is a stationary link between patterns and local climate, that is, no within-type change, and climate change manifests only as between-type change. In this way a constant parametrization of a WGN conditioned on WPs can be used. To test this assumption, different trend analyses are performed.

For trend detection the nonparametric two-sided Mann-Kendall test (Kendall, 1938), which is based on a rank correlation coefficient, is applied ($p < 0.05$). The magnitude of change is derived from Sen's slope (Sen, 1968, equation (1)):

$$\beta = \text{median}\left(\frac{x_n - x_m}{n - m}\right) \quad ; \text{for all } n > m; x_n, x_m = \text{time series values in years } n, m \tag{1}$$

Trend magnitudes are known to be sensitive to the selection of start and end points of the investigation period. In particular in our analysis, it might be expected to have periods incorporated in the data that are mainly influenced by anthropogenic climate change, while this effect is not clearly evident in other periods (i.e., might be masked by internal variability or natural forcings). To eliminate any potential effect of a fixed time period, trend analyses for multiple periods are performed. Statistical tests are applied to every time period with a minimum length of 31 years resulting in trend matrices indicating the magnitude and (field) significance of multiple trends within the period 1900/1901 – 2010. Each pixel/cell of the triangular matrix represents the trend results for a combination of a particular start year (x axis) and end year (y axis). In the case of variables derived at each climate station separately (e.g., pattern mean temperature), each pixel represents the spatial average across all stations.

To account for possible autocorrelation in the time series, which might distort the result of the Mann-Kendall trend test, a block bootstrap approach as proposed by Khaliq et al. (2009) is applied. This approach is based on resampling a correlated time series such that the correlation structure is preserved (i.e., taking blocks of data that are longer than the number of significantly autocorrelated time lags). The test statistic (here Kendall's tau) is derived from the resampled time series. Repeating this procedure a large number of times (1,000) results in a simulated distribution of the test statistic. If the test statistic of the original series lies in the tails of this distribution, it is unlikely to obtain that value from a time series with the same correlation structure but no temporal trend; thus, the trend of the original time series is judged to be unaffected by autocorrelation.

When performing trend analyses on multiple stations within a region, the question arises whether the observed number of trends is significantly larger than what might be found by chance only. Applying the block bootstrapping for all stations simultaneously, thus preserving the spatial correlation between neighboring stations, field significance can be evaluated as well. The number of trends in the shuffled time series is counted and compared to the observed number. If the observed number lies in the tails of the distribution of simulated number of trends, this is judged to be field significant. Performing this analysis for each individual period and highlighting the field significant periods gives contours of field significance as presented, for example, in Figure 5.

For the detection of changes in pattern characteristics, trend analyses (i.e., Mann-Kendall test and Sen's slope) are performed on annual mean values of pattern frequency, seasonality, and persistence ("between-type changes") and on pattern-specific annual mean climatic values of all stations ("within-type changes"). Seasonality is expressed as the average date of pattern occurrence, taking into account the circular nature of dates when calculating trends (i.e., considering that the difference between day 365 and day 1 is +1 rather than −364) by using an approach of Bayliss and Jones (1993) that converts the date into an angular value. Patterns that occur mainly in spring and autumn show two distinct peaks of seasonal occurrence, which are analyzed separately for shifts in seasonality. For aggregating trend results of climatic values across all stations, trend magnitudes were spatially averaged across all stations and field significance is calculated as described above.

3.3. Relative Share of Between- and Within-Type Changes

For relating the change in a certain meteorological variable to changes in pattern frequency, the "hypothetical trend" approach as proposed by, for example, Huth (2001) is applied, comparing the WP-induced trend to the observed trend (Fleig et al., 2015). A hypothetical time series of daily (e.g., precipitation) values of a climate

station is constructed by replacing each original daily value with the station-specific long-term monthly mean value of the respective WP associated with that day (for a detailed description see Fleig et al., 2015). The ratio of the linear trend (i.e., Sen's slope) in the WP-induced (i.e., hypothetical) series to the linear trend in the observed time series is then computed. It can potentially take values from $-\infty$ to ∞. The meaning of some selected values are as follows:

$R > 0$: Pattern-induced and original trend are of the same sign.
$R < 0$: Pattern-induced and original trend are of opposite sign.
$R = 1$: Original trend is completely related to the trend in pattern frequency.
$0 < R < 1$: Within-type trends are of the same sign as between-type trends.
$R > 1$: Within-type trends are of the opposite sign to between-type trends.

The hypothetical trend approach is able to identify opposing trends, for example, in case a changed frequency of patterns would lead to an increase in precipitation, but a decreasing trend was observed due to drying of the corresponding patterns. The method is applied for multiple periods, calculating long-term monthly pattern mean values separately for each period. The trend ratio only gives meaningful results for significant trends (Cahynová & Huth, 2010). Although trend magnitudes of original and WP-induced trends are presented for all stations, trend ratios are only calculated for stations with significant ($p < 0.05$) original trends.

4. Results

4.1. Linking WPs to Large-Scale Circulation Modes

Results of the correlation analysis (Figure 3) clearly reveal that WPs (particularly those triggering moist or dry conditions over the target region) result from the superposition and regional manifestation of large-scale pressure modes and thus represent major atmospheric processes, such as the formation of cyclonic and anticyclonic circulation patterns and the associated deflection of large-scale heat and moisture fluxes. Moisture conditions during winter are strongly related with the state of the EAWR and the SCA. WPs showing a strong positive correlation with EAWR and SCA are associated with blocking over central Europe and Scandinavia, respectively. Monthly frequencies of dry WPs 36, 14, 40, and 21 show positive (and partially statistically significant) correlations with EAWR, which indicates an increased occurrence of dry WPs during its positive state. The same applies for SCA (positive correlations for WPs 14, 37, and 12). Moist WPs (characterized by negative pressure anomalies over northern and/or central Europe and a consequential cyclonic circulation) show an inverse relationship. A clear influence of the NAO on the frequency of dry and moist WPs during winter is not detectable, slight positive correlations with NAO are found for the dry WPs 36 and 40, and negative correlations are detected for the moist WP 17. During spring, summer, and autumn the relationship between WP frequencies and large-scale atmospheric conditions is less pronounced. For the moist WPs 2, 18, and 35 a negative relationship with NAO is detected.

The trend analysis of teleconnection indices for multiple periods (Appendix, Figure A1) indicates significant positive trends of EA and NAO for the period after 1948, particularly for the winter season. Likewise, for EAWR trends are positive (although not statistically significant) during most periods. For wintertime SCA a slight negative trend is detected. These trends might be interpreted as a consequence of an intrinsic multidecadal variability of wintertime circulation modes (Hurrell, 1995; Krichak & Alpert, 2005; Selten et al., 1999; Wang et al., 2012), which however might explain observed trends of WP frequencies (and local scale observations) to a certain extent.

4.2. Between-Type Changes

Changes in pattern frequency are detected for many patterns in distinct periods and with varying trend direction and magnitude (Figure 4; for full set of WPs see supporting information). For wet winter patterns 24 and 17 slightly decreasing frequencies of up to 0.05% per year (season and precipitation intensity are depicted by icons in the subplots) are detected in most periods since the 1950s and increasing trends in periods ending around 1970 and 1980. Both patterns are negatively correlated with EAWR, and recent changes of WP frequencies are clearly related to positive trends of the winter EAWR index after 1950. Wet winter WPs 30 and 23, featuring a strong negative relationship with SCA, show increasing frequencies (only statistically significant for WP 30) since the 1950s, which is also in agreement with observed trends of the SCA index. For both WPs long-term increases in frequency of up to 0.05% are detected. Both feature very similar temperature and humidity patterns, with a low pressure anomaly over Scandinavia (see Figure 2), which is slightly shifted

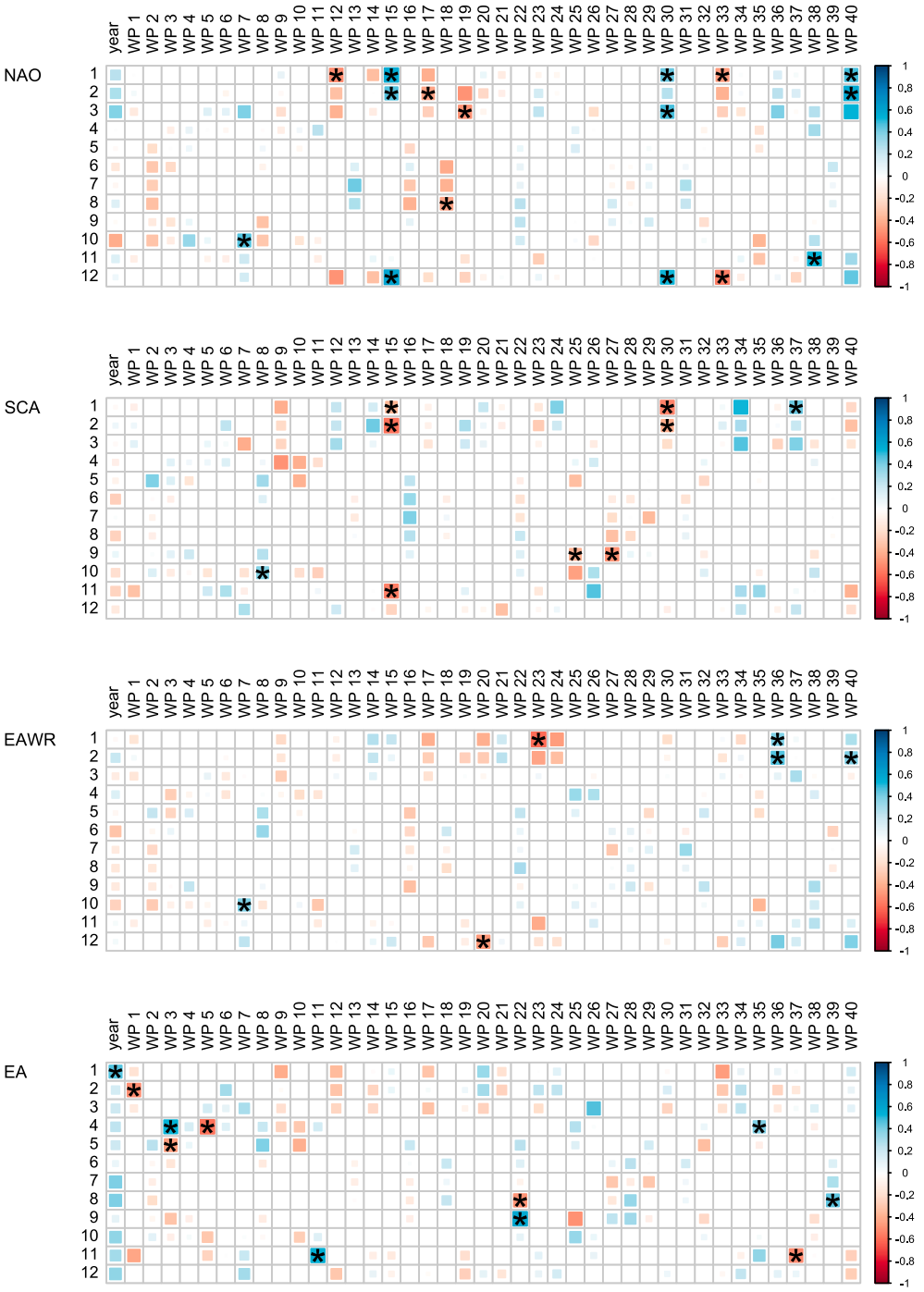

Figure 3. Correlation of pattern frequency and averaged index of selected large-scale atmospheric circulation modes. Correlations are only shown if the pattern has a maximal occurrence of at least 20% in the respective months. Asterisks indicate significant correlations.

southward in WP 23. This similarity results in rather similar mean local climate (see Appendix in Murawski et al., 2016). Dry winter WPs, which are positively correlated with the EAWR pattern (36, 14, and 40), show slightly positive frequency trends in recent periods (increasing frequency in WP 40 is detected for many periods ending between 1990 and 2010 with magnitudes of up to 0.1% per year) and decreasing frequency ending in the 1970/1980s. Although WPs 36 and 14 feature rather similar mean sea level pressure (msl) and humidity patterns, they clearly differ in temperature. Thus, this pair of WPs would be prone for capturing temperature

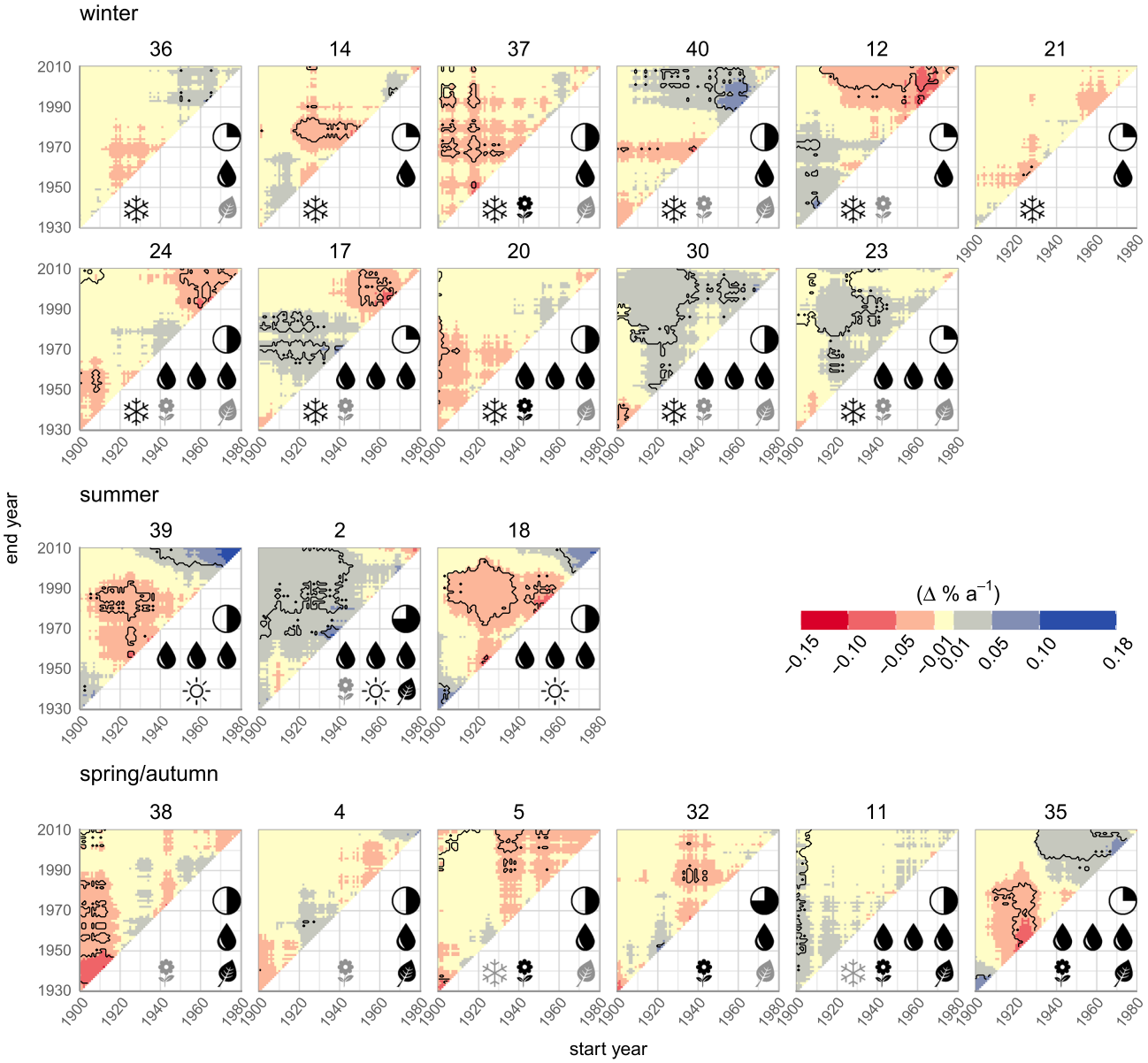

Figure 4. Multiple trends of pattern frequency (dry and wet patterns only). Each value of the top triangle denotes the trend magnitude of a specific period, given by its start year (horizontal axis) and end year (vertical axis). Black contours enclose time periods with statistically significant trends (Mann-Kendall test, $p < 0.05$). Icons in bottom right corner of panels denote season(s) of pattern occurrence (snowflake, DJF; flower, MAM; Sun, JJA; leaf, SON; black, main season; gray, few occurrences), mean daily precipitation (1 drop, [0, 1.25] mm d^{-1}; 2 drops, (1.25, 4] mm d^{-1}; 3 drops, (4, 7.4] mm d^{-1}), and frequency of pattern (one quarter of circle filled black, pattern occurs in [0, 2]% of days; two quarters filled, (2, 3]%; three quarters filled, (3, 3.5]%; all filled, (3.5, 3.8]%). (Icons (drop and seasons) made by Freepik and Icon Works from https://www.flaticon.com).

changes by a mere exchange of these two, but their trends in frequency are in the same direction for most periods. Dry winter WPs 40 and 12 show almost opposite frequency trends: decreasing (increasing) trends for periods ending between 1990 and 2010 with particularly higher magnitudes around 1960, and increasing (decreasing) trends until the 1970s. While WP 40 might be interpreted as a superposition of a positive NAO and a positive EAWR pattern, which favors blocking over central Europe, WP 12 rather occurs under negative NAO conditions in combination with a positive state of SCA (see Figure 3). Again, the observed frequency trends of both WPs follow those of relevant large-scale circulation modes after 1950. For WP 37, being strongly positively correlated with SCA, slightly decreasing frequency is detected for several periods starting around 1910 and 1920 or ending in 1970 or 1980.

Wet summer patterns 39 and 18 became more frequent in recent decades (more than 0.1% per year for WP 39) but show alternating trend direction in earlier periods (negative in the middle of the century and positive again between 1900 and 1930) but no trends persisting over the whole century. Although trends in the frequency of these WPs are quite similar throughout the century, they have notably different pressure anomalies (see Figure 2). While WP 18 is dominated by a low pressure anomaly over central Europe, the pressure anomaly is less pronounced and rather located in the southeast of Europe in WP 39, which is furthermore associated with higher temperature and humidity than WP 18. Both WPs are positively correlated with EA, which features a strong interdecadal variability with mainly positive trends during recent decades. WP 18 is also strongly negatively correlated with NAO.

While most spring/autumn patterns do not show significant trends in recent decades, for wet WP 35 increasing frequency is detected for periods beginning after 1930 and ending after 2000, which is in agreement with positive trends of the positively correlated EA pattern in spring and autumn. In contrast, the negatively correlated WP 5 (dry) shows slightly (but mostly not significant) decreasing frequency after 1930. For wet WP 11 (also positively correlated with EA) only few increasing trends of low magnitude are detected, mostly for periods starting around 1900. For dry WP 38, which is positively correlated with NAO and EAWR, decreasing trends in frequency are only detected for periods starting between 1900 and 1920.

In summary, the trend patterns of WP frequencies are found to follow the trends (or more likely the long-term variability) of northern hemispheric circulation modes. This is most pronounced during winter season where dry (wet) conditions are related with the positive (negative) manifestation of EAWR and/or SCA. Those dry patterns related with a positive EAWR state show significant positive trends during recent decades; for patterns related to a positive SCA a frequency decrease is detected. Reversal relationships are found for wet WPs.

The seasonality of patterns (Appendix, Figure B1; for full set of WPs see supporting information) changes only little with usually less than 1 day change per year. For dry and wet winter patterns many weak short-term trends are found, usually of alternating direction and being close to 0 for century-long periods. Some general trend patterns are evident in association with large-scale pressure modes; for example, WP 40 (and 12) is positively (negatively) correlated with NAO and shows tendencies toward later (earlier) occurrence of up to 1 day per year for the most recent decades and earlier (later) occurrence of the same magnitude for periods roughly ending before 1990. For the wet winter pattern 20 earlier occurrence of up to 2 days per year is detected for periods ending before 1970 and starting after 1950, and later occurrence of the same magnitude is detected for periods in between. The seasonality of wet summer patterns exhibits hardly any significant trends and is of low magnitude only. For spring/autumn a clear tendency of earlier occurrence in spring of up to 1 day per year (translating to a shift of 1 month for a 30 year period) is evident for recent periods. Simultaneously, the autumn peak of many patterns shifted to later occurrence in recent periods. However, the latter is less pronounced than the shift in spring.

The majority of patterns does not exhibit a change in persistence, and only very few show long-term but weak changes (Appendix, Figure B2; for full set of WPs see supporting information). Increasing persistence in long-term periods is found for wet summer pattern 2, although the trend weakened and is not significant in recent decades. This is in general consistent with the observed increases in frequency of this pattern. Dry winter WP 14 shows a significant increase in persistence for periods starting in the 1960s and lower persistence for periods ending around 1980. This suggests a local minimum in persistence of this relatively dry winter pattern in this decade. The magnitude of these trends average around 0.05 and −0.03 days per year, respectively, which sums up to a change of 1.5 (−0.9) days for 30 years. Considering an average persistence of this pattern of almost 3 days, this change translates to a relatively significant proportion (average persistence of patterns varies between 1.4 and 3 days). In general, most signals detected in pattern frequency are found in persistence as well. This synchronization indicates that changes in pattern frequency are mostly caused by changes in persistence, which are likewise related to the interdecadal variability of the northern hemispheric circulation, as represented by the NAO, SCA, EA, and EAWR teleconnection indices.

4.3. Within-Type Changes

Multiple trend analyses on pattern-specific mean climatic values are presented in Figures 5 and 6 and Appendix, Figures B3 and B4 (for panels with full set of patterns see supporting information). For T_{av} (Figure 5) many dry winter patterns show a warming trend until the 1980s and a cooling trend for recent periods

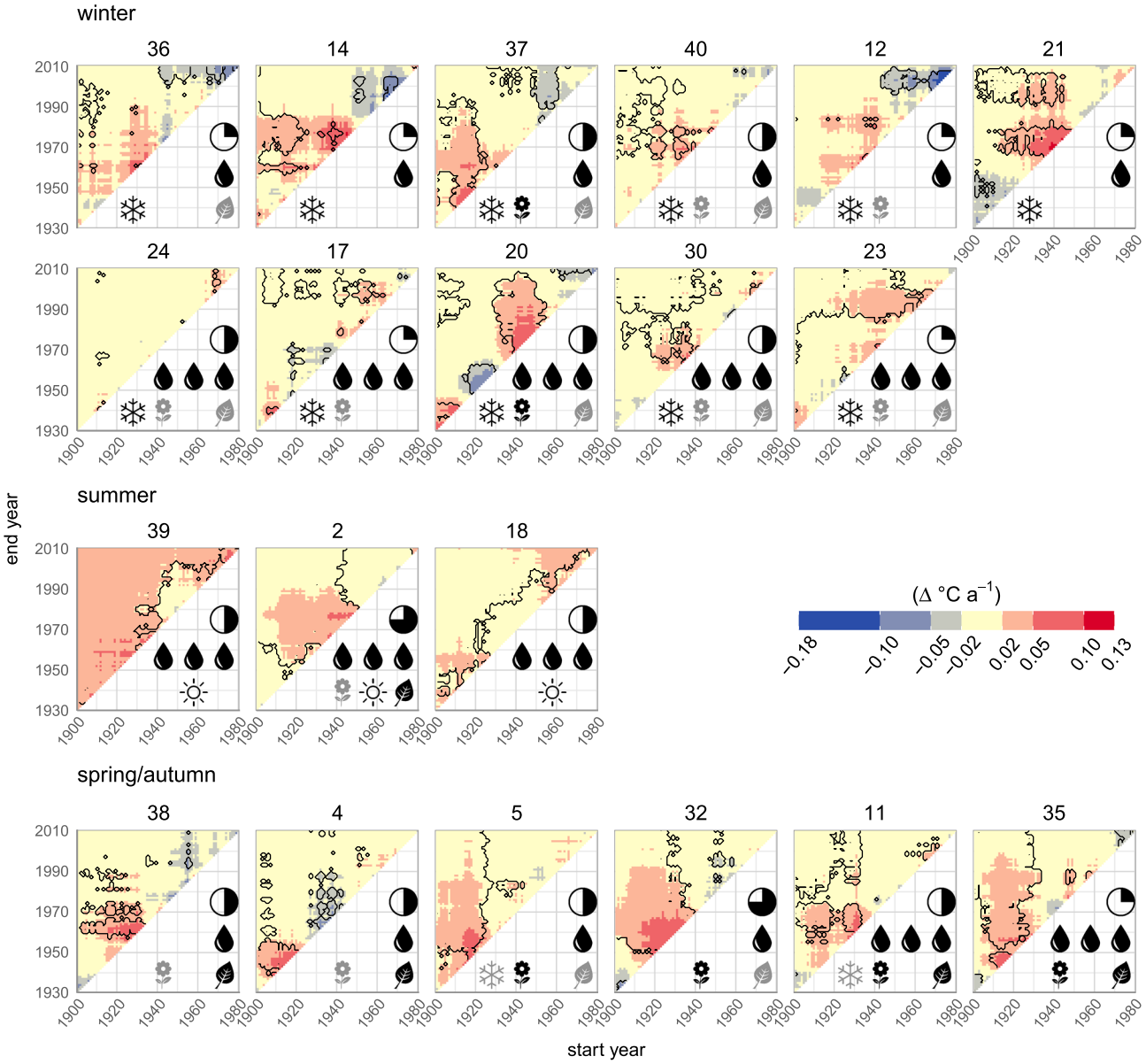

Figure 5. Multiple trends of pattern mean daily temperature (dry and wet patterns only). Plot as in Figure 4, except that black contours enclose time periods with field significant trends ($p < 0.05$).

(WPs 36, 14, 37, and 12). The cooling is not pronounced for wet winter patterns (except WP 20), but warming trends are detected for some short periods in the middle of the century (WPs 20 and 23). All wet summer patterns exhibit long-term significant warming but of low magnitudes of maximum 0.05 K. Spring/autumn patterns reveal warming trends in the beginning of the century which do not persist in recent decades.

Trends in precipitation (Figure 6) are most pronounced (i.e., highest absolute magnitudes) in wet patterns, while for dry patterns almost no significant trends were detected and if so, their magnitudes are close to 0. Wet winter patterns show long-term wetting trends of up to 0.05 mm per year; however, all of them (except WP 30) indicate nonsignificant drying trends in very recent periods. Wet summer pattern 39 shows significant long-term decreasing precipitation, while wet summer WP 18 indicates opposite trends. In spring/autumn only for WP 35 significant wetting is detected for periods starting between the 1920s and 1950.

Most trends in shortwave radiation (Appendix, Figure B3) are rather short-term, and only few sustain during the whole century. This suggests the presence of decadal fluctuations in shortwave radiation associated with

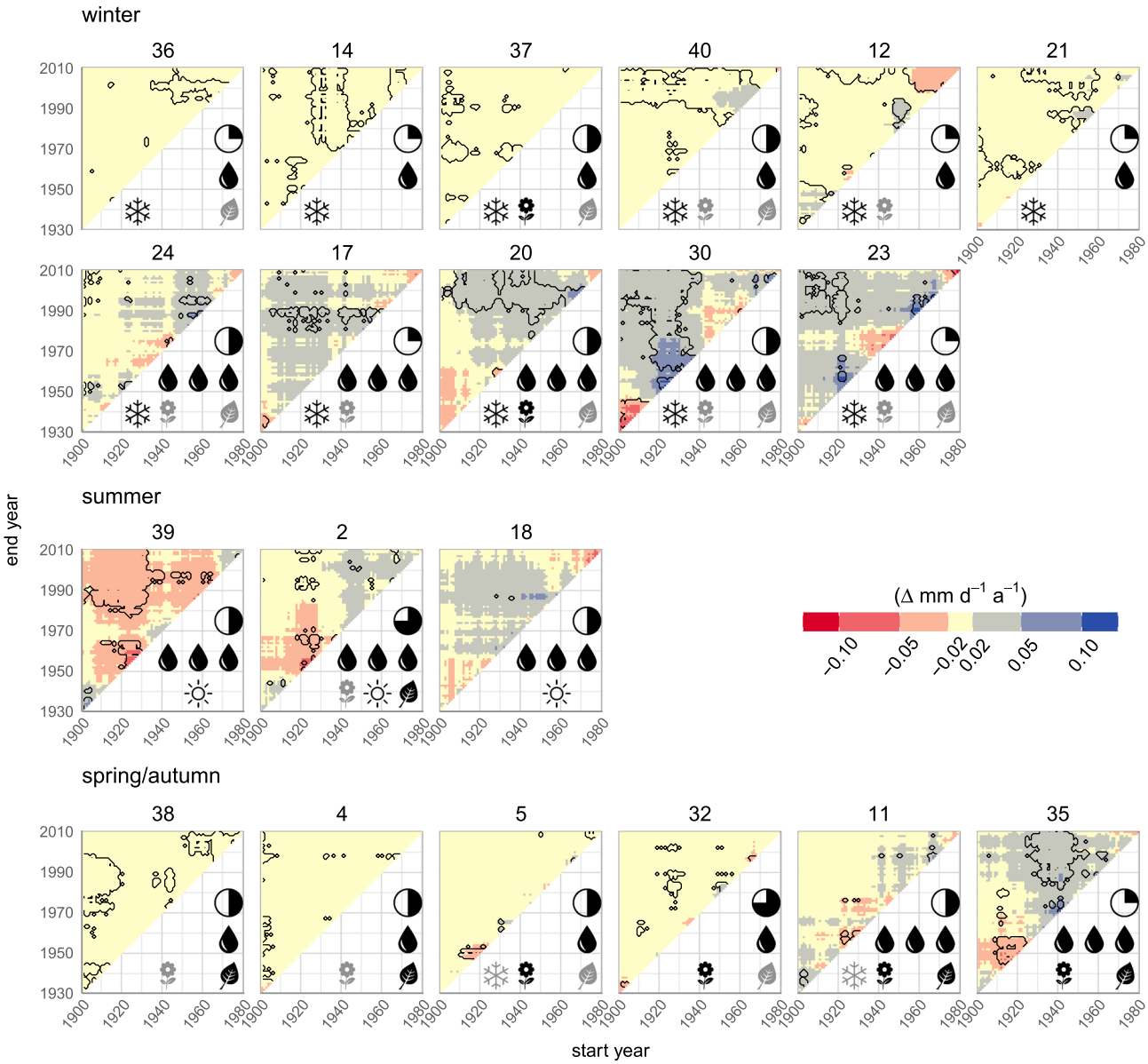

Figure 6. Multiple trends of pattern mean daily precipitation (dry and wet patterns only). As in Figure 5.

various WPs. Especially for winter, trends, if present at all, prevail only in very few periods. In spring/autumn many wet or dry patterns show increasing trends for periods ending around 1960 and decreasing trends for periods starting around 1940. For summer WPs 39 and 2 long-term increasing trends in shortwave radiation are detected, which weakened or switched sign in more recent decades.

For relative humidity (Appendix, Figure B4) very heterogeneous trends are found with periods of positive and negative trends in most patterns. Especially for wet summer and dry spring/autumn patterns trends in relative humidity are parallel to those in shortwave radiation. This also suggests strongly pronounced fluctuations in WP-related humidity.

4.4. Relative Share of Between- and Within-Type Changes

Trends in annual climatic variables averaged over the catchment are analyzed for multiple periods (Figures 7 and 8, top row). Trends in temperature variables are positive over nearly all periods starting after 1950 or ending after 2000 in all seasons (less pronounced in autumn). Increased warming of more than 0.03°C a^{-1}

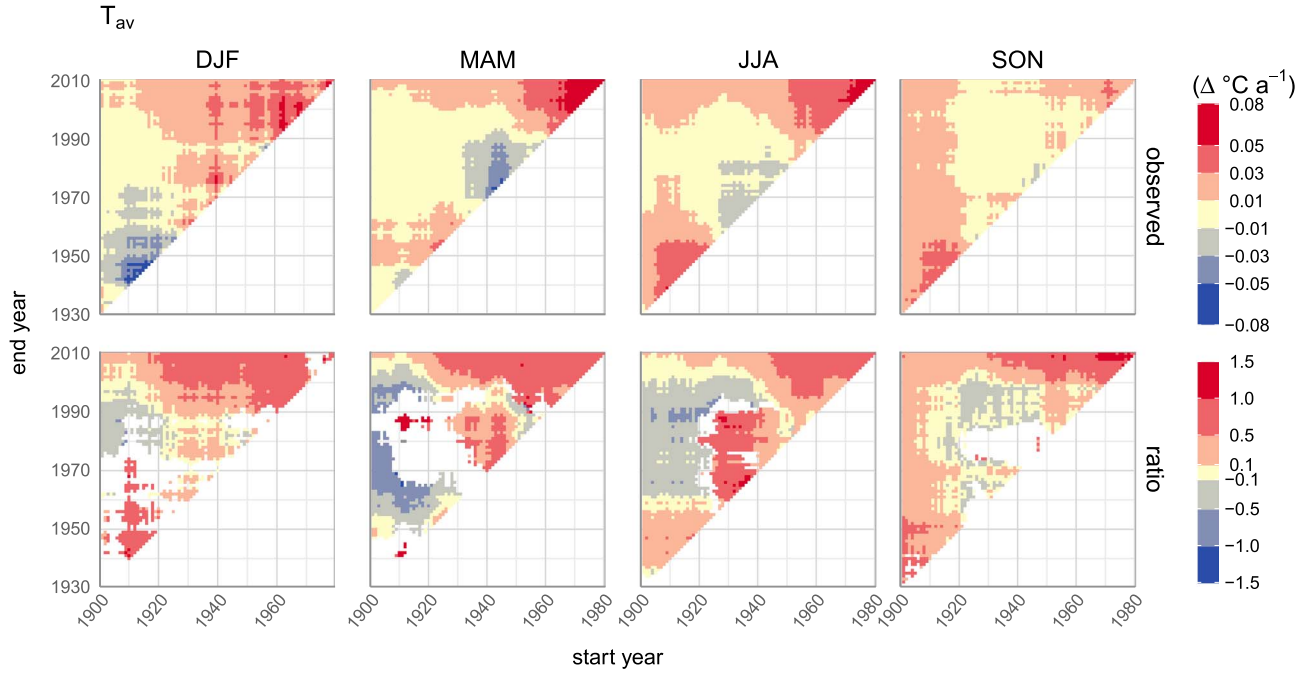

Figure 7. (top row) Trends in catchment average mean daily temperature for all seasons and (bottom row) associated ratio of WP-induced and original trend slopes (see section 3.3). Ratios are only calculated for stations with significant original trends and presented as averages across stations. Gaps appear for periods with no significant trends.

since the 1960s is detected. A pronounced cooling is found for winter for periods ending before 1950 and for spring for periods starting around 1940. WP-induced trends (Figures 7 and 8, bottom row) follow the observed trends to a large degree and explain 50% to almost 100%, especially for recent periods with high magnitudes of change. Periods with negative slope ratios (i.e., WP-induced trends are of opposite sign to the original trends) occur only for periods with almost no trends.

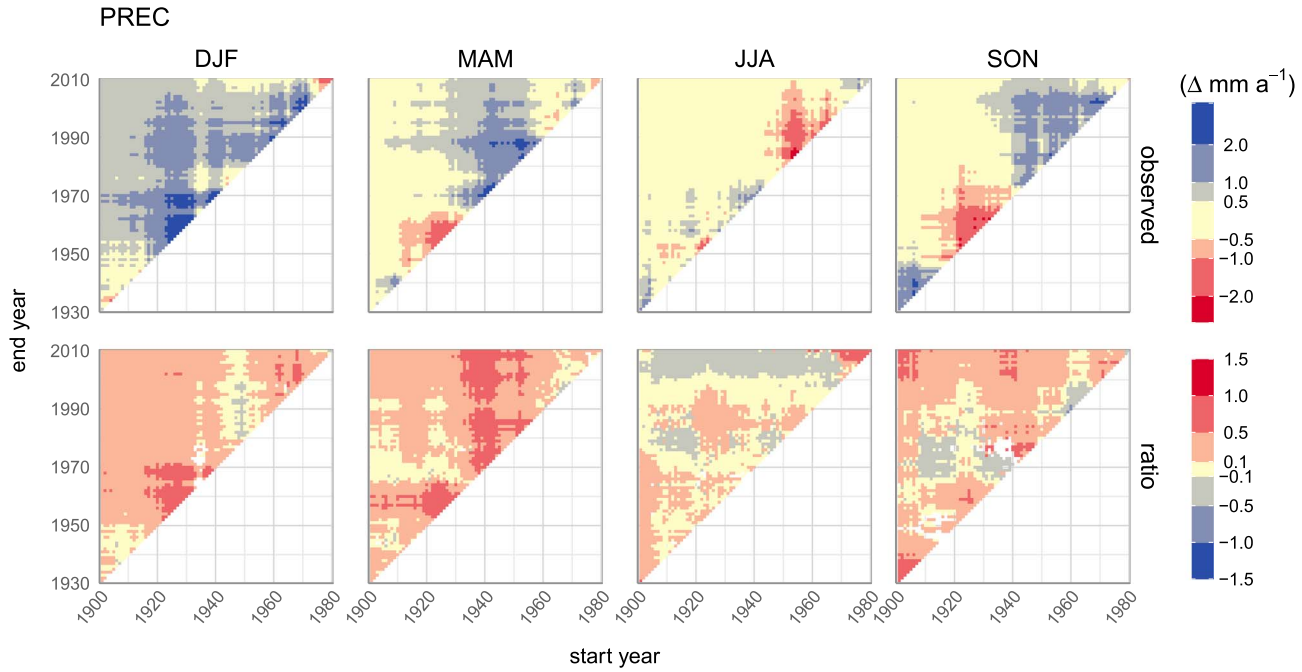

Figure 8. Trends in catchment average daily precipitation for all seasons. As in Figure 7.

Trends in precipitation are detected for winter in almost all periods (magnitude of change usually less than 1 mm per year and up to more than 2 mm per year only for very few periods). For spring and autumn increasing precipitation was mainly found for periods starting after 1940, whereas changes in summer precipitation are close to 0 and only pronounced negative for few periods starting in the 1950s. Up to 50% of the changes in precipitation, although only weak, can be explained by WP-induced changes. For periods with more pronounced precipitation changes (e.g., winter, periods around 1930–1960, and spring, periods starting around 1940) more than half of the change is attributable to between-type changes.

Changes in shortwave radiation and relative humidity (Appendix, Figures B5 and B6) show decadal variations in trend direction, which is most pronounced in spring and summer. WP-induced changes are usually of not more than half the magnitude of original trends, indicating some substantial proportion of within-type changes.

5. Discussion and Conclusions

In this paper we analyzed the "optimal" WP classification presented in Murawski et al. (2016) for trends within and between patterns. The climatic properties of the patterns will be used to parametrize a WGN to serve as a downscaling tool in a climate change attribution study. The assumption for this WGN-based approach is that changes in local climate variables can be explained by changes in the pattern frequency, seasonality, and persistence. This assumption was examined here by applying trend analyses to pattern characteristics and the mean climatic properties of patterns over multiple periods. Between-type and within-type changes analyzed here cannot be interpreted as dynamic and thermodynamic changes, because temperature and specific humidity are included in the classification. The classification of Murawski et al. (2016) aims at optimizing the amount of explained variance rather than to purely separate between dynamic and thermodynamic predictors. However, the analysis shows that such kind of classification is superior in terms of the envisaged application. WP classifications are common in the literature (e.g., Hewitson & Crane, 2006; Kalkstein et al., 1987) and are different from the circulation pattern classifications that use only pressure variables (Huth et al., 2008).

Trends in the frequency of patterns were found in most patterns, although they were usually not uniform across all periods but might change direction between decades and smooth out for longer periods. Some increases in frequency were detected particularly in winter patterns that are associated with high precipitation. It was shown that trends of central European WPs in recent decades follow the variability of large-scale teleconnection indices, such as the NAO, SCA, EA, and EAWR. Thus, the WP classification is capable of depicting major northern hemispheric circulation modes and associated anomalies of moisture and heat fluxes.

Changes in persistence were usually less pronounced but are in agreement with observed changes of WP frequencies. For pattern seasonality a tendency, albeit small, in recent decades toward earlier occurrence of wet spring patterns was found, representing increased precipitation during snow melt and thus potentially increased flood severity.

The hypothetical trend analysis shows that a substantial portion of changes in precipitation and particularly temperature at 490 stations within the Rhine catchment can be assigned to changes of the WP composition. These periods coincide with the highest observed warming, thus clearly emphasizing the importance of between-type changes for overall temperature trends, if thermodynamic variables are considered. This relation is already indicated in Corti et al. (1999) but seems to not hold true anymore after 1995 (Yiou et al., 2007); however, conclusions on the periods after 1995 are not possible from our analyses (using at least 30 year periods until 2010 at the latest). Explained trend ratios were especially high during winter season, where moist and dry conditions are strongly related to variations of the EAWR and the SCA. The significant link between large-scale circulation modes and WP frequencies as well as the high potential of the WP classification to explain observed trends of surface variables support the utilization of a modeling chain, including WP classification, a stochastic WGN, and a distributed catchment model, to investigate the variability and change of flood probabilities in the Rhine catchment.

However, some WPs are characterized by heterogeneous local weather conditions and high ratios of within-type trends. A long-term warming trend was found for all summer patterns. Such a clear signal was not evident for winter patterns where trends were weaker and not persistent on long periods. Winter patterns

rather showed a cooling in the last decades and slight warming before. Many spring/autumn patterns showed a strong warming trend until about 1970. Trends for pattern-specific shortwave radiation and relative humidity were dominated by decadal fluctuations. These results hint toward the high variability of trend detection results depending on the selected time period and emphasize the usefulness of assessing multiple periods.

We found that within-type changes dominated in periods with overall small changes in temperature. In the literature different percentages for within-type temperature changes were reported depending on the selected period and methodology. Küttel et al. (2011) found 70% within-type change of winter temperature for central Europe when comparing the first and second halves of the 20th century. Cahynová and Huth (2016) and Huth (2001) summarized that trends in summer temperature (1949–1980) at two Czech Republic stations were unrelated to frequency changes, while a warming trend in winter could be assigned to changes in pattern frequency. Also, Philipp et al. (2007) found higher amounts of between-type temperature changes since 1850 for winter (59%) than for summer (33.9%) and again evidence for high within-type variability. Cahynová and Huth (2010) concluded that internal changes were "responsible for a major part of the observed climatic trends in spring, summer, and autumn; but also in winter for variables other than temperature." In contrast to the previous studies, our results suggest a much stronger role of between-type trends (75–100%) for periods with notable temperature changes revealed by multiple period analyses. This advantage can clearly be assigned to the optimized WP classification (Murawski et al., 2016), which included temperature as a characteristic variable additional to the pressure fields. We show indeed that observed changes in temperature and precipitation can be related to WPs (if thermodynamic variables are included), which finally allows the use of a WGN-based downscaling for the past period for analysis of flood changes. This is only possible, because the classification accounts for both dynamical and thermodynamical changes. Global circulation models are known to satisfactorily reproduce large-scale climate anomalies and associated fluxes of heat and moisture. However, surface climate observations, particularly precipitation, are highly affected by local-scale site conditions and thus are not reliably simulated. The results clearly indicate that a downscaling approach based on WPs is feasible and that trends of near-surface temperature and precipitation during the 20th century can be assigned to changing large-scale atmospheric conditions.

Although considering the specific humidity for WP classification, we were not able to significantly improve the amount of changes in relative humidity that is due to changes in pattern frequency. Cahynová and Huth (2010) found near-zero (summer) to only 20% of between-type changes in humidity, which is clearly supported by our results. Changes in shortwave radiation were associated with changes in pattern frequency by a slightly higher proportion than humidity (around 50% for periods with decreasing trends) but were nevertheless highly influenced by within-type changes. Decreasing shortwave radiation in periods starting around 1940 and ending around 1990 might be related to high aerosol loading in the atmosphere: Andronova and Schlesinger (2000) found a cooling of near-surface temperature between 1940 and 1970 being explained by volcanic activities and partly by solar irradiance, while Walter and Schönwiese (2003) found a particularly strong cooling effect of sulfur dioxide at a global scale in this period. The same cooling effect was reported in an updated study by Schönwiese et al. (2010), who found almost zero trends in temperature for 1945–1975 along with a strong increase in forcing by sulfate aerosols. The cooling found in our data is only weak, possibly being masked by other effects. The high aerosol loading, however, is clearly visible in decreasing trends of shortwave radiation in these periods.

Observed precipitation changes were represented by WP-induced trends in nearly all periods; that is, observed and WP-induced trends were of the same direction and slope ratios were positive. However, WP-induced trends accounted for somewhat more than half of the observed changes only in periods ending in the 2000s; earlier periods were dominated by within-type changes. Comparable amounts of within-type changes were also found by Küttel et al. (2011) (60% of winter precipitation), however, for other periods. A general trend direction for a specific season was not evident—the two wettest summer patterns (18 and 39) showed rather opposite within-type trend directions.

In the present paper, being a follow-up from Murawski et al. (2016) where an "optimal" classification of WPs was developed, we thoroughly analyzed the underlying assumptions for a WP-WGN based downscaling approach. Contrary to previous studies, we found a higher portion of observed trends in temperature and precipitation being explained by pattern frequency. This would justify an application of a pattern-conditioned

WGN, although a certain portion of uncertainty (i.e., nonassignable amount of changes) is inherent to the method. Low explained share of humidity and shortwave radiation trends is a clear limitation. However, for the purpose of flood change attribution to anthropogenic climate change, the role of the latter two variables for higher floods is believed to be minor and can be investigated in a sensitivity study. Hence, the use of WP-WGN based downscaling can be acceptable for flood change attribution if properly interpreted. Further, it must be noted that the WP approach is calibrated with reanalysis data, which impedes the analysis of future climate change based on global circulation models. Global change will most likely alter the large-scale fluxes of thermodynamic variables and might induce conditions that have not been observed during the reanalysis period. Thus, for the investigation of future climate change impacts, more complex statistical techniques (such as regression approaches, possibly combined with the suggested WP classification) should be considered.

Appendix A: Circulation Modes

Large-scale atmospheric circulation modes are analyzed for trends on multiple periods. Trends across periods can be related to trends in weather patterns as presented, for example, in Figure 4.

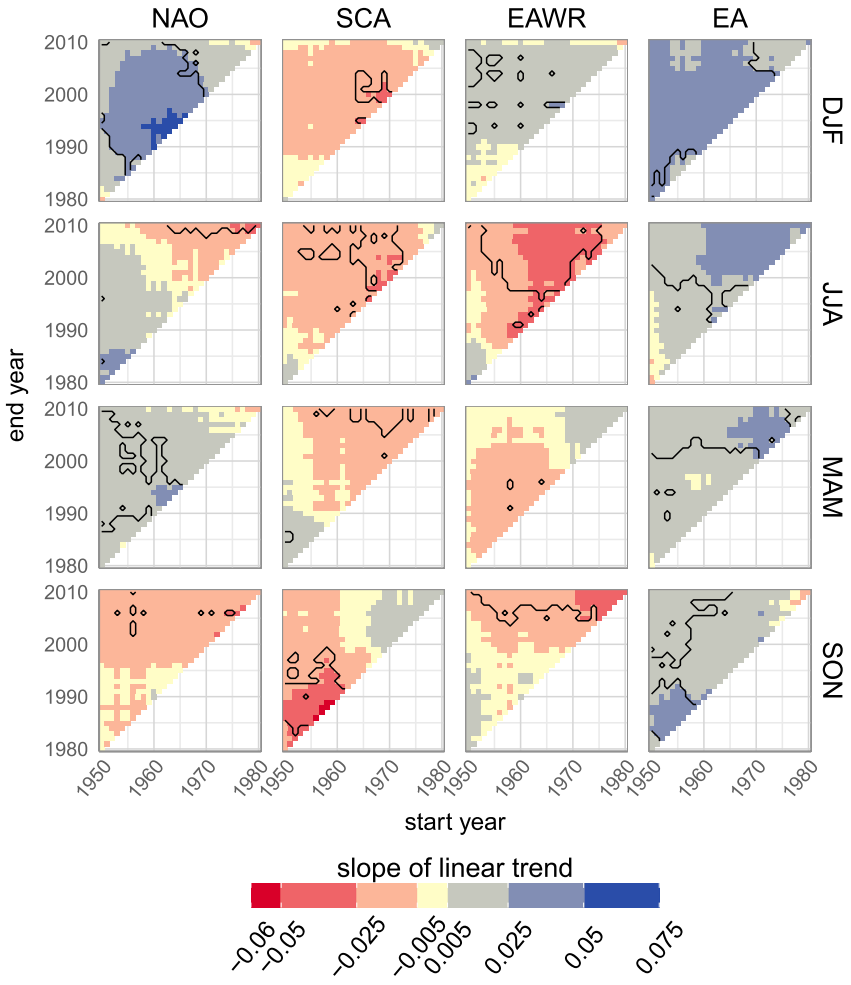

Figure A1. Multiple trends of large-scale atmospheric circulation modes. Note that start of axes differs from other trend plots.

Appendix B: Trend Results

Results of multiple trend analyses on seasonality and persistence of patterns, as well as on relative humidity and shortwave radiation, are presented here.

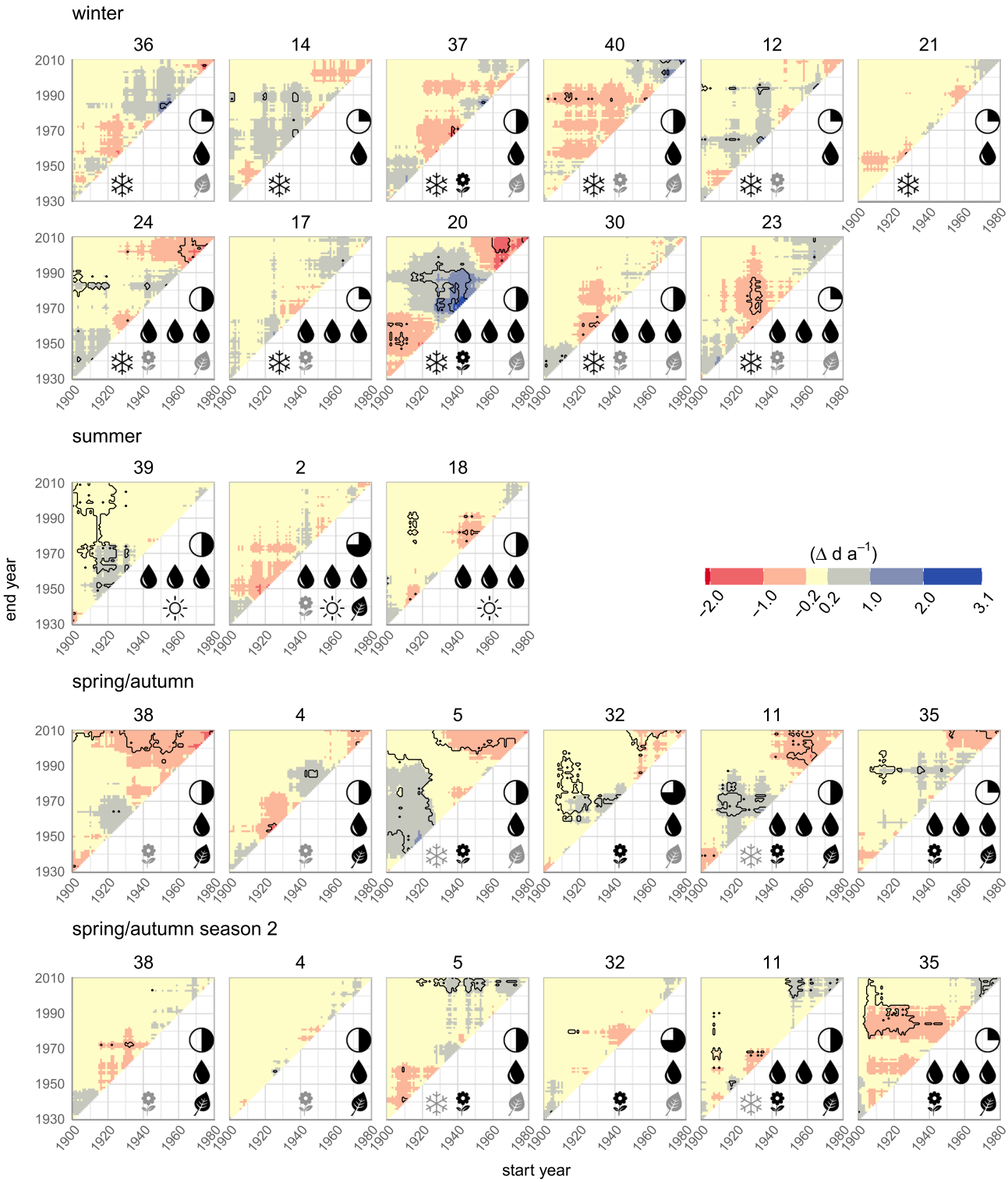

Figure B1. Multiple trends of pattern seasonality (dry and wet patterns only). As in Figure 4.

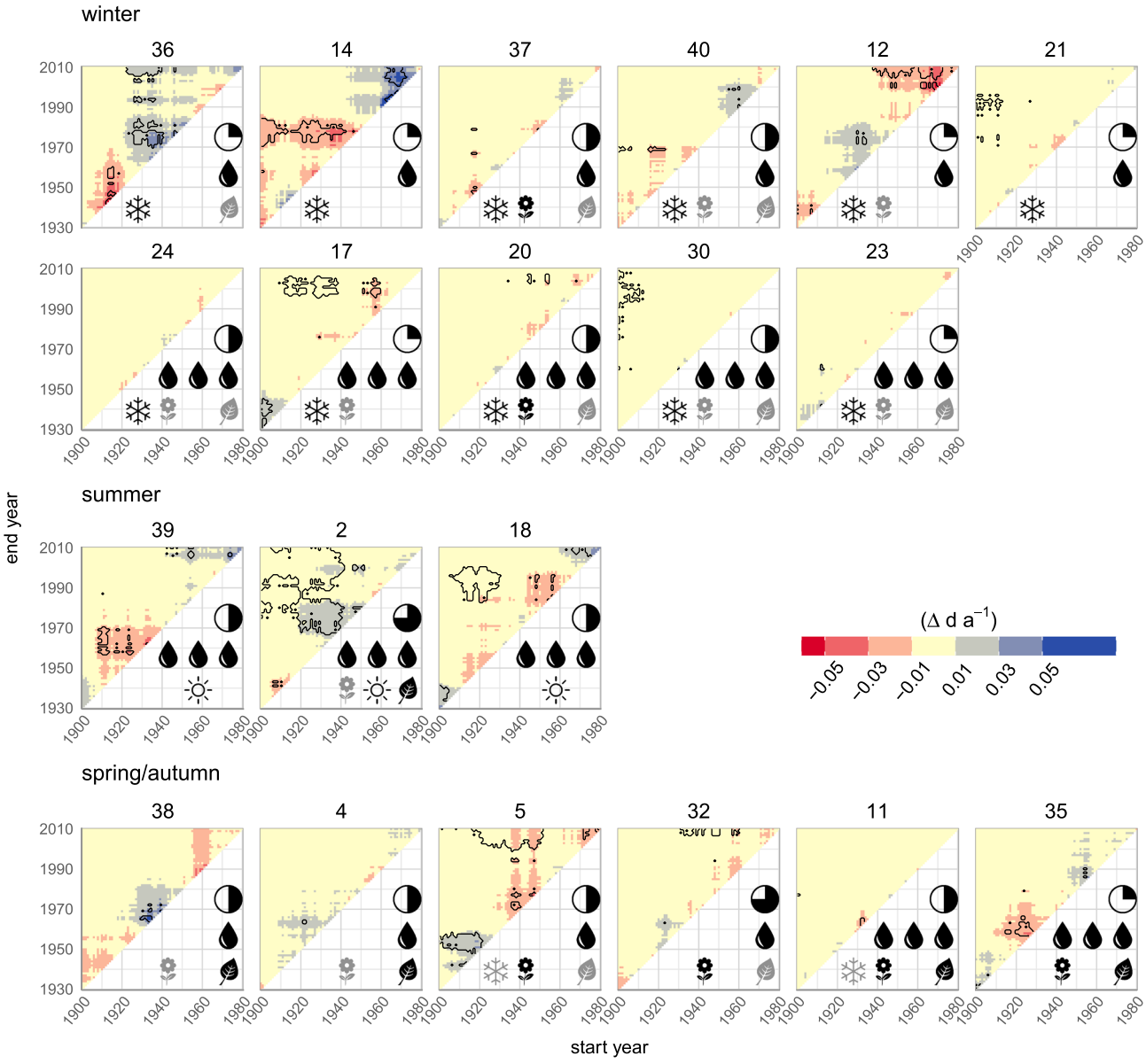

Figure B2. Multiple trends of pattern persistence (dry and wet patterns only). As in Figure 4

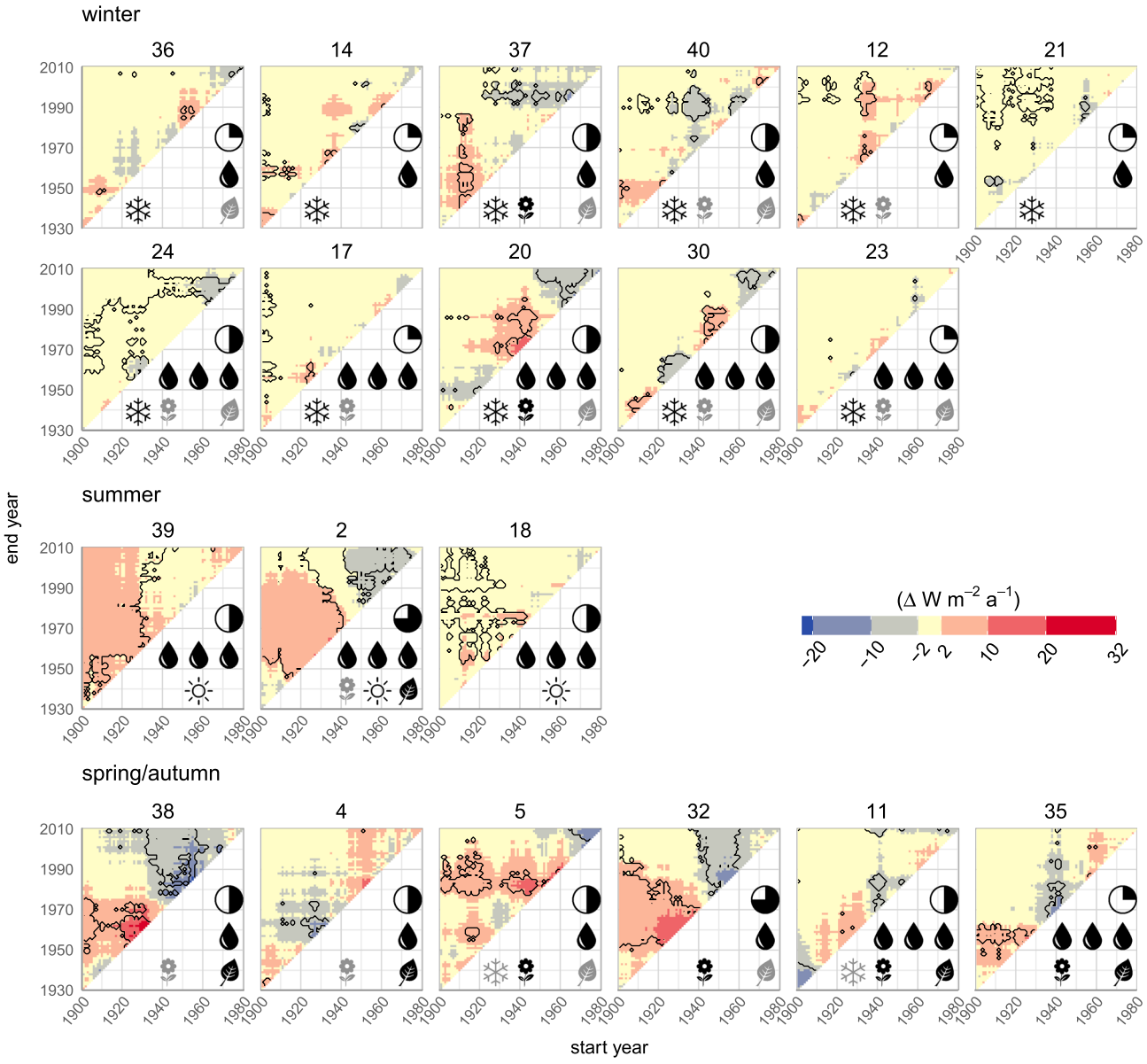

Figure B3. Multiple trends of pattern mean daily shortwave radiation (dry and wet patterns only). As in Figure 5.

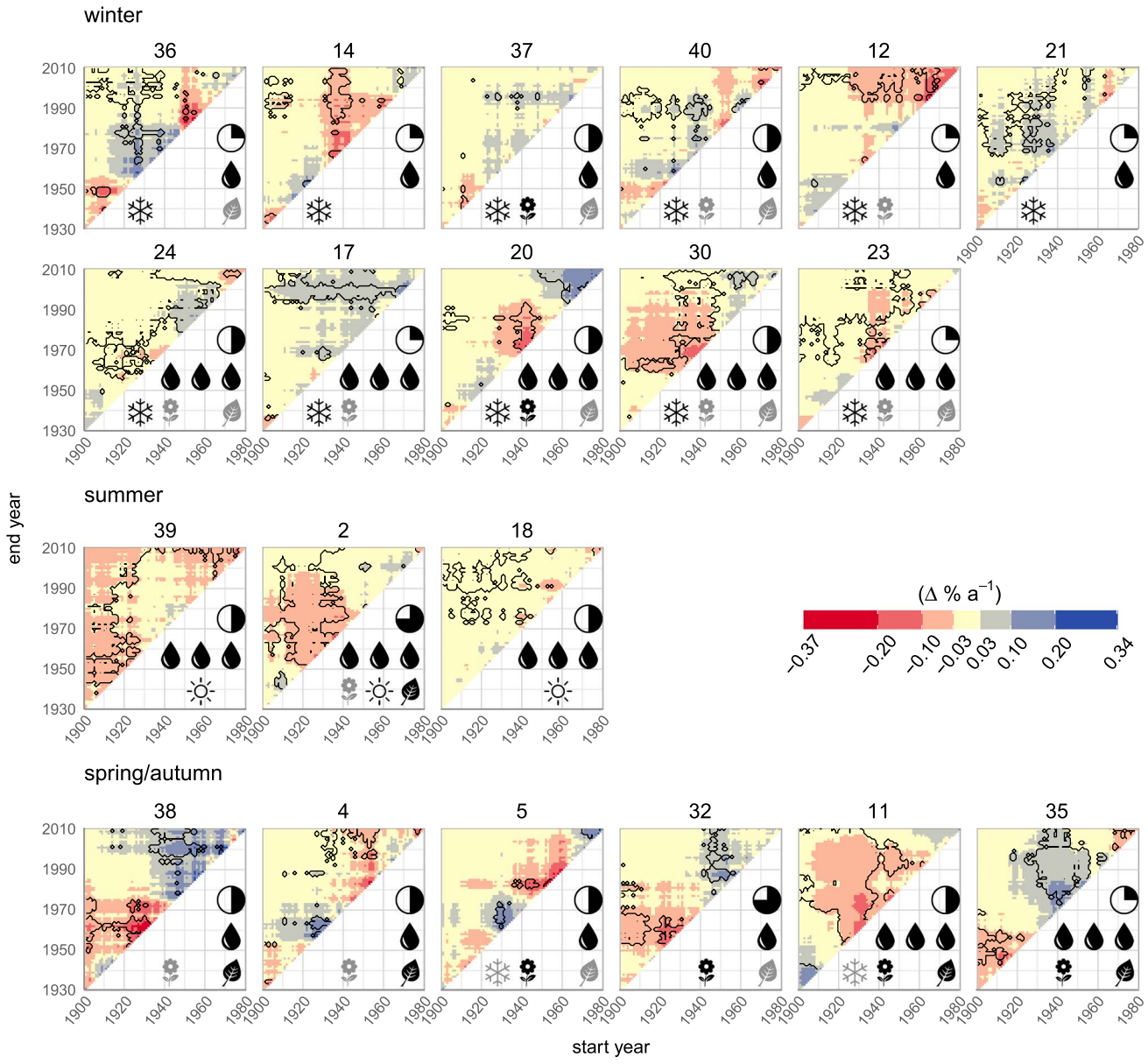

Figure B4. Multiple trends of pattern mean daily relative humidity (dry and wet patterns only). As in Figure 5.

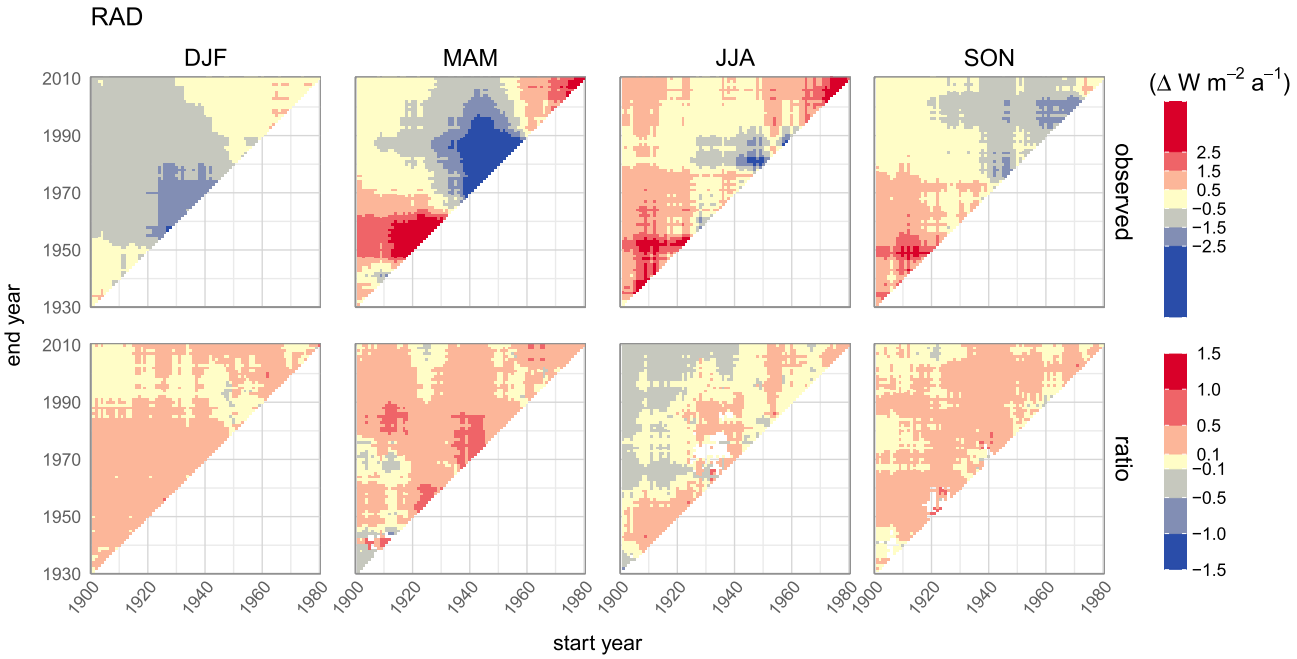

Figure B5. (top row) Trends in catchment average mean daily shortwave radiation for all seasons and (bottom row) associated ratio of WP-induced and original trend slopes (see section 3.3). Ratios are only calculated for stations with significant original trends and presented as averages across stations. Gaps appear for periods with no significant trends.

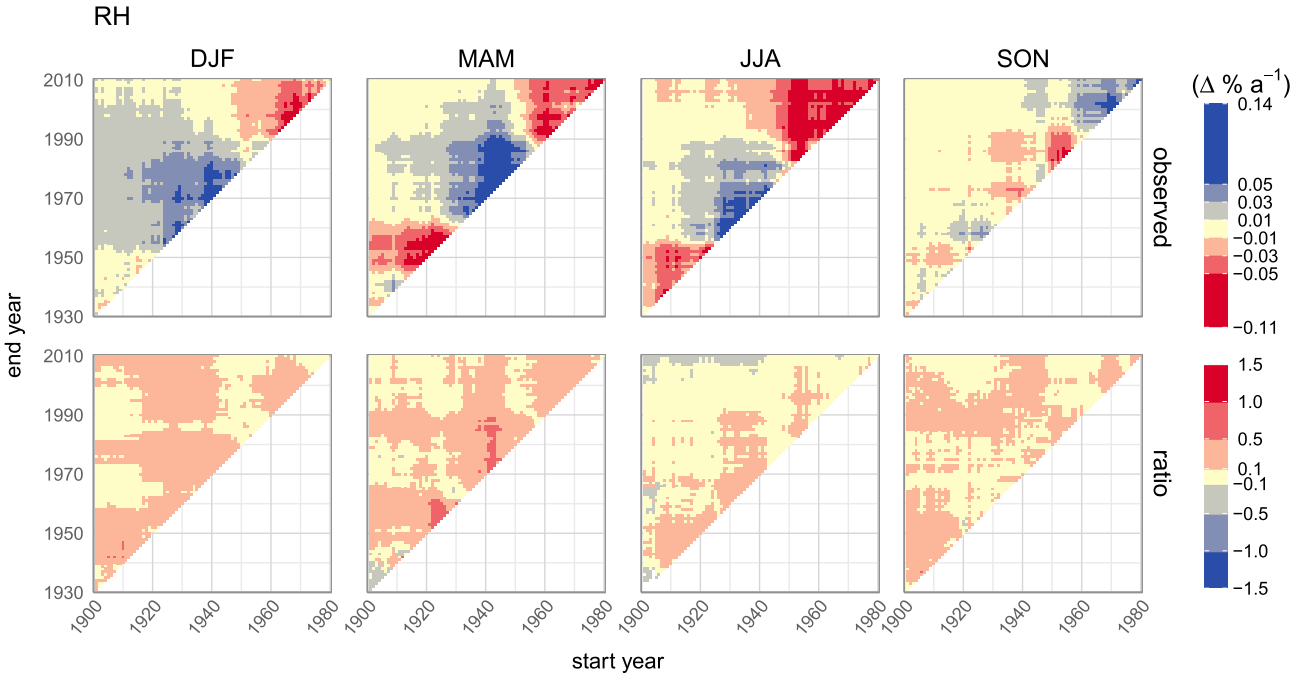

Figure B6. Trends in catchment average daily relative humidity for all seasons. As in Figure B5.

Acknowledgments
We thank three anonymous reviewers for their suggestions and comments on this manuscript. We gratefully appreciate the provision of data by the national meteorological services of Germany, Austria, and Switzerland, kindly provided and processed by the Potsdam-Institute for Climate Impact Research (PIK). A. Murawski acknowledges funding by Climate KIC. The climate station data are owned by PIK and are not publicly accessible. The weather pattern classification catalog used here is provided in the supporting information along with netcdf files of the centroids of the patterns.

References

Andronova, N. G., & Schlesinger, M. E. (2000). Causes of global temperature changes during the 19th and 20th centuries. *Geophysical Research Letters*, *27*, 2137–2140.

Barnston, A. G., & Livezey, R. E. (1987). Classification, seasonality and persistence of low-frequency atmospheric circulation patterns. *Monthly Weather Review*, *115*, 1083–1126.

Bayliss, A. C., & Jones, R. C. (1993). Peaks-over-threshold flood database: summary statistics and seasonality. Report 121. Wallingford, UK: Institute of Hydrology.

Beck, C., Jacobeit, J., & Jones, P. D. (2007). Frequency and within-type variations of large-scale circulation types and their effects on low-frequency climate variability in central Europe since 1780. *International Journal of Climatology*, *27*, 473–491. https://doi.org/10.1002/joc.1410

Brezowsky, H., & Hess, P. (1952). *Katalog der Großwetterlagen Europas, Berichte der Deutscher Wetterdenst in der US-Zone*.

Bueh, C., & Nakamura, H. (2007). Scandinavian pattern and its climatic impact. *Quarterly Journal of the Royal Meteorological Society*, *133*, 2117–2131.

Cahynová, M., & Huth, R. (2010). Circulation vs. climatic changes over the Czech Republic: A comprehensive study based on the COST733 database of atmospheric circulation classifications. *Physics and Chemistry of the Earth*, *35*, 422–428. https://doi.org/10.1016/j.pce.2009.11.002

Cahynová, M., & Huth, R. (2016). Atmospheric circulation influence on climatic trends in Europe: An analysis of circulation type classifications from the COST733 ue. *International Journal of Climatology*, *36*, 2743–2760. https://doi.org/10.1002/joc.4003

Comas-Bru, L., & McDermott, F. (2014). Impacts of the EA and SCA patterns on the European twentieth century NAO–winter climate relationship. *Quarterly Journal of the Royal Meteorological Society*, *140*, 354–363.

Corti, S., Molteni, F., & Palmer, T. (1999). Signature of recent climate change in frequencies of natural atmospheric circulation regimes. *Nature*, *398*, 799–802.

Elshamy, M. E., Wheater, H. S., Gedney, N., & Huntingford, C. (2006). Evaluation of the rainfall component of a weather generator for climate impact studies. *Journal of Hydrology*, *326*, 1–24. https://doi.org/10.1016/j.jhydrol.2005.09.017

Enke, W., Schneider, F., & Deutschländer, T. (2005). A novel scheme to derive optimized circulation pattern classifications for downscaling and forecast purposes. *Theoretical and Applied Climatology*, *82*, 51–63. https://doi.org/10.1007/s00704-004-0116-x

Fatichi, S., Ivanov, V. Y., & Caporali, E. (2011). Simulation of future climate scenarios with a weather generator. *Advances in Water Resources*, *34*, 448–467. https://doi.org/10.1016/j.advwatres.2010.12.013

Fleig, A. K., Tallaksen, L. M., James, P., Hisdal, H., & Stahl, K. (2015). Attribution of European precipitation and temperature trends to changes in synoptic circulation. *Hydrology and Earth System Sciences*, *19*, 3093–3107. https://doi.org/10.5194/hess-19-3093-2015

Fowler, H., Kilsby, C., O'Connell, P., & Burton, A. (2005). A weather-type conditioned multi-site stochastic rainfall model for the generation of scenarios of climatic variability and change. *Journal of Hydrology*, *308*, 50–66. https://doi.org/10.1016/j.jhydrol.2004.10.021

Fowler, H. J., Kilsby, C. G., & O'Connell, P. E. (2000). A stochastic rainfall model for the assessment of regional water resource systems under changed climatic condition. *Hydrology and Earth System Sciences*, *4*, 263–281. https://doi.org/10.5194/hess-4-263-2000

Haberlandt, U., Belli, A., & Bárdossy, A. (2015). Statistical downscaling of precipitation using a stochastic rainfall model conditioned on circulation patterns—An evaluation of assumptions. *International Journal of Climatology*, *35*, 417–432. https://doi.org/10.1002/joc.3989

Hewitson, B. C., & Crane, R. G. (2006). Consensus between GCM climate change projections with empirical downscaling: Precipitation downscaling over South Africa. *International Journal of Climatology*, *26*, 1315–1337. https://doi.org/10.1002/joc.1314

Hurrell, J. W. (1995). Decadal trends in the North Atlantic Oscillation: Regional temperatures and precipitation. *Science*, *269*, 676–678.

Huth, R. (2001). Disaggregating climatic trends by classification of circulation patterns. *International Journal of Climatology*, *21*, 135–153.

Huth, R., Beck, C., Philipp, A., Demuzere, M., Ustrnul, Z., Cahynová, M., … Tveito, O. E. (2008). Classifications of atmospheric circulation patterns. *Annals of the New York Academy of Sciences*, *1146*, 105–152. https://doi.org/10.1196/annals.1446.019

Jacobeit, J., Wanner, H., Luterbacher, J., Beck, C., Philipp, A., & Sturm, K. (2003). Atmospheric circulation variability in the North-Atlantic-European area since the mid-seventeenth century. *Climate Dynamics*, *20*, 341–352. https://doi.org/10.1007/s00382-002-0278-0

Kalkstein, L. S., Tan, G., & Skindlov, J. A. (1987). An evaluation of three clustering procedures for use in synoptic climatological classification. *Journal of Climate and Applied Meteorology*, *26*, 717–730. https://doi.org/10.1175/1520-0450(1987)026<0717:AEOTCP>2.0.CO;2

Kendall, M. G. (1938). A new measure of rank correlation. *Biometrika*, *30*, 81–93.

Khaliq, M., Ouarda, T., Gachon, P., Sushama, L., & St-Hilaire, A. (2009). Identification of hydrological trends in the presence of serial and cross correlations: A review of selected methods and their application to annual flow regimes of Canadian rivers. *Journal of Hydrology*, *368*, 117–130. https://doi.org/10.1016/j.jhydrol.2009.01.035

Kilsby, C., Jones, P., Burton, A., Ford, A., Fowler, H., Harpham, C., … Wilby, R. (2007). A daily weather generator for use in climate change studies. *Environmental Modelling & Software*, *22*, 1705–1719. https://doi.org/10.1016/j.envsoft.2007.02.005

Kim, J., Ivanov, V. Y., & Fatichi, S. (2016). Climate change and uncertainty assessment over a hydroclimatic transect of Michigan. *Stochastic Environmental Research and Risk Assessment*, *30*, 923–944. https://doi.org/10.1007/s00477-015-1097-2

Krichak, S. O., & Alpert, P. (2005). Decadal trends in the east Atlantic–west Russia pattern and Mediterranean precipitation. *International Journal of Climatology*, *25*, 183–192.

Küttel, M., Luterbacher, J., & Wanner, H. (2011). Multidecadal changes in winter circulation-climate relationship in Europe: Frequency variations, within-type modifications, and long-term trends. *Climate Dynamics*, *36*, 957–972. https://doi.org/10.1007/s00382-009-0737-y

Lu, Y., Qin, X. S., & Mandapaka, P. V. (2015). A combined weather generator and K-nearest-neighbour approach for assessing climate change impact on regional rainfall extremes. *International Journal of Climatology*, *35*, 4493–4508. https://doi.org/10.1002/joc.4301

Maraun, D., Wetterhall, F., Ireson, A. M., Chandler, R. E., Kendon, E. J., Widmann, M., … Thiele-Eich, I. (2010). Precipitation downscaling under climate change: Recent developments to bridge the gap between dynamical models and the end user. *Reviews of Geophysics*, *48*, RG3003. https://doi.org/10.1029/2009RG000314

Murawski, A., Bürger, G., Vorogushyn, S., & Merz, B. (2016). Can local climate variability be explained by weather patterns? A multi-station evaluation for the Rhine basin. *Hydrology and Earth System Sciences*, *20*, 4283–4306. https://doi.org/10.5194/hess-20-4283-2016

Österle, H. (2001). Reconstruction of daily global radiation for past years for use in agricultural models. *Physics and Chemistry of the Earth, Part B: Hydrology, Oceans and Atmosphere*, *26*, 253–256. https://doi.org/10.1016/S1464-1909(00)00248-3

Österle, H., Gerstengarbe, F., & Werner, P. (2006). Ein neuer meteorologischer Datensatz für Deutschland, 1951-2003. Potsdam: Potsdam Institute for Climate Impact Research.

Österle, H., Gerstengarbe, F.-W., & Werner, P. C. (2016). *Die Elbe im Globalen Wandel, chap. 2.2 Ein Meteorologischer Datensatz für Deutschland, 1951–2003* (pp. 81–84). Stuttgart, Germany: Schweizerbart Science Publishers.

Österle, H., Werner P. C., & Gerstengarbe F. W. (2006). Qualitätsprüfung, Ergänzung und Homogenisierung der täglichen Datenreihen in Deutschland, 1951-2003: Ein neuer Datensatz, *Deutsche Klimatagung. Klimatrends: Vergangenheit und Zukunft*. München (Munich).

Philipp, A. (2009). Comparison of principal component and cluster analysis for classifying circulation pattern sequences for the European domain. *Theoretical and Applied Climatology*, *96*, 31–41. https://doi.org/10.1007/s00704-008-0037-1

Philipp, A., Della-Marta, P. M., Jacobeit, J., Fereday, D. R., Jones, P. D., Moberg, A., & Wanner, H. (2007). Long-term variability of daily North Atlantic-European pressure patterns since 1850 classified by simulated annealing clustering. *Journal of Climate*, *20*, 4065–4095. https://doi.org/10.1175/jcli4175.1

Poli, P., Hersbach, H., Tan, D., Dee, D., Thepaut, J.-N., Simmons, A., … Fisher, M. (2013). The data assimilation system and initial performance evaluation of the ECMWF pilot reanalysis of the 20th-century assimilating surface observations only (ERA-20C) (ERA Report Series 14). European Centre for Medium-Range Weather Forecasts (ECMWF). Reading, UK.

Schönwiese, C.-D., Walter, A., & Brinckmann, S. (2010). Statistical assessments of anthropogenic and natural global climate forcing. An update. *Meteorologische Zeitschrift*, *19*, 3–10.

Selten, F. M., Haarsma, R., & Opsteegh, J. (1999). On the mechanism of North Atlantic decadal variability. *Journal of Climate*, *12*, 1956–1973.

Sen, P. K. (1968). Estimates of the regression coefficient based on Kendall's Tau. *Journal of the American Statistical Association*, *63*, 1379–1389. https://doi.org/10.1080/01621459.1968.10480934

Shepherd, T. G. (2014). Atmospheric circulation as a source of uncertainty in climate change projections. *Nature Geoscience*, *7*, 703–708. https://doi.org/10.1038/ngeo2253

Steinschneider, S., & Brown, C. (2013). A semiparametric multivariate, multisite weather generator with low-frequency variability for use in climate risk assessments. *Water Resources Research*, *49*, 7205–7220. https://doi.org/10.1002/wrcr.20528

Steirou, E., Gerlitz, L., Apel, H., & Merz, B. (2017). Links between large-scale circulation patterns and streamflow in central Europe: A review. *Journal of Hydrology*, *549*, 484–500. https://doi.org/10.1016/j.jhydrol.2017.04.003

Taylor, K. E., Stouffer, R. J., & Meehl, G. A. (2012). An overview of CMIP5 and the experiment design. *Bulletin of the American Meteorological Society*, *93*, 485–498. https://doi.org/10.1175/bams-d-11-00094.1

te Linde, A. H., Aerts, J. C. J. H., Bakker, A. M. R., & Kwadijk, J. C. J. (2010). Simulating low-probability peak discharges for the Rhine basin using resampled climate modeling data. *Water Resources Research*, *46*, W03512. https://doi.org/10.1029/2009WR007707

Uvo, C. B. (2003). Analysis and regionalization of northern European winter precipitation based on its relationship with the North Atlantic Oscillation. *International Journal of Climatology*, *23*, 1185–1194.

Walter, A., & Schönwiese, C.-D. (2003). Nonlinear statistical attribution and detection of anthropogenic climate change using a simulated annealing algorithm. *Theoretical and Applied Climatology*, *76*, 1–12.

Wang, Y.-H., Magnusdottir, G., Stern, H., Tian, X., & Yu, Y. (2012). Decadal variability of the NAO: Introducing an augmented NAO index. *Geophysical Research Letters*, *39*, L21702. https://doi.org/10.1029/2012GL053413

Widmann, M., & Schär, C. (1997). A principal component and long-term trend analysis of daily precipitation in Switzerland. *International Journal of Climatology*, *17*, 1333–1356. https://doi.org/10.1002/(SICI)1097-0088(199710)17:12<1333::AID-JOC108>3.0.CO;2-Q

Yiou, P., Vautard, R., Naveau, P., & Cassou, C. (2007). Inconsistency between atmospheric dynamics and temperatures during the exceptional 2006/2007 fall/winter and recent warming in Europe. *Geophysical Research Letters*, *34*, L21808. https://doi.org/10.1029/2007GL031981